Surface Science 102 (1981) 99–117

THE ADSORPTION OF CO, O_2, AND H_2 ON Pt(100)-(5 × 20)

M.A. BARTEAU, E.I. KO and R.J. MADIX
Department of Chemical Engineering, Stanford University, Stanford, California 94305, USA

Received 18 March 1980; accepted for publication 24 July 1980

The adsorption/desorption characteristics of CO, O_2, and H_2 on the Pt(100)-(5 × 20) surface were examined using flash desorption spectroscopy. Subsequent to adsorption at 300 K, CO desorbed from the (5 × 20) surface in three peaks with binding energies of 28, 31.6 and 33 kcal $gmol^{-1}$. These states formed differently from those following adsorption on the Pt(100)-(1 × 1) surface, suggesting structural effects on adsorption. Oxygen could be readily adsorbed on the (5 × 20) surface at temperatures above 500 K and high O_2 fluxes up to coverages of 2/3 of a monolayer with a net sticking probability to ssaturation of $\geqslant 10^{-3}$. Oxygen adsorption reconstructed the (5 × 20) surface, and several ordered LEED patterns were observed. Upon heating, oxygen desorbed from the surface in two peaks at 676 and 709 K; the lower temperature peak exhibited atrractive lateral interactions evidenced by autocatalytic desorption kinetics. Hydrogen was also found to reconstruct the (5 × 20) surface to the (1 × 1) structure, provided adsorption was performed at 200 K. For all three species, CO, O_2, and H_2, the surface returned to the (5 × 20) structure only after the adsorbates were completely desorbed from the surface.

1. Introduction

The adsorption characteristics of simple molecules on various crystal planes of platinum have been the subject of numerous studies in the literature of the past decade [1]. The motivations of such studies have been several. First, as platinum is an excellent catalyst with applications to both hydrocarbon cracking and reforming, a better understanding of adsorption and simple rate processes on these surfaces is of interest. Second, the crystal planes of platinum have been reported to exhibit marked anisotropies for adsorption of simple molecules [2], and a fundamental understanding of these effects is still lacking. Third, the oxidation of simple molecules such as CO and H_2 on platinum surfaces has received a great deal of attention; it is apparent from past studies that the adsorption characteristics and binding states of the reactants may significantly affect the kinetics of the reaction [3–5], and further investigations are needed in order to elucidate the reaction mechanisms.

It is well known that the Pt(100) surface undergoes a reconstruction from a (1 × 1) to a (5 × 20) LEED structure, [6], which appears to be the thermodynamically favored structure for the clean surface [7]. However, adsorption of species

such as CO or NO induces a reversal of reconstruction to the (1 × 1) structure. A substantial structural dependence also has been reported for the sticking probability of oxygen on the Pt(100) surface: oxygen may be adsorbed on the (1 × 1) structure with an initial sticking probability of 0.1 [8], whereas the initial sticking probability on the (5 × 20) surface has been reported to be 4×10^{-4} [9], and numerous other workers have reported *no* adsorption of oxygen on this surface.

A similar structural dependence has also been reported for the adsorption of hydrogen on the Pt(100) surface: the sticking probability of hydrogen on the (1 × 1) surface has been reported to be three orders of magnitude greater than that on the (5 × 20) surface at 300 K [1]. Likewise, although the sticking probability for CO adsorption does not exhibit a large structural dependence, the sequence of LEED patterns observed with increasing CO coverage is dependent upon the unitial surface structure even though CO adsorption reverses the reconstruction of the (5 × 20) surface [1].

The purpose of the present study was to examine the adsorption and desorption characteristics of the simple molecules CO, O_2, and H_2 on the Pt(100)-(5 × 20) surface in order to provide some insight into the reactions of these species on the surface – in particular, the oxidation of CO to CO_2. Detailed kinetic studies of this reaction were also performed, and will be reported in a later communication [5].

2. Experimental

The experimental apparatus has been described in detail elsewhere [10]. The vacuum chamber contained 4-grid optics for LEED, a cylindrical mirror analyzer and Mg Kα X-ray source for AES and XPS, and a UTI 100C quadrupole mass spectrometer for TPRS. The sample was suspended by a polycrystalline Pt wire spotwelded to the backside of the sample. The Pt wire was suspended ~8 cm off axis from a manipulator located along the central vertical axis of the chamber. This allowed rotation of the sample in the plane perpendicular to the manipulator. The sample was cooled by means of a copper braid connected to a liquid nitrogen reservoir external to the chamber. A planar tungsten filament was suspended ~2 mm behind the sample. Power was supplied to the filament by means of a variable DC power supply. The sample could be heated linearly by radiation from the filament between 300 and 800 K or maintained at constant temperature within this range by manual control of the power supplied to the filament. The sample could also be heated to 1700 K by electron bombardment heating. A potential of –800 V was applied to the sample, and the heating filament was used to provide electrons for bombardment. The sample temperature was monitored by means of a Pt–Pt/Rh thermocouple spotwelded to the back of the sample.

The sample was initially cleaned by argon ion bombardment. Small amounts of calcium were removed by annealing the sample to 1700 K. Carbon was removed by

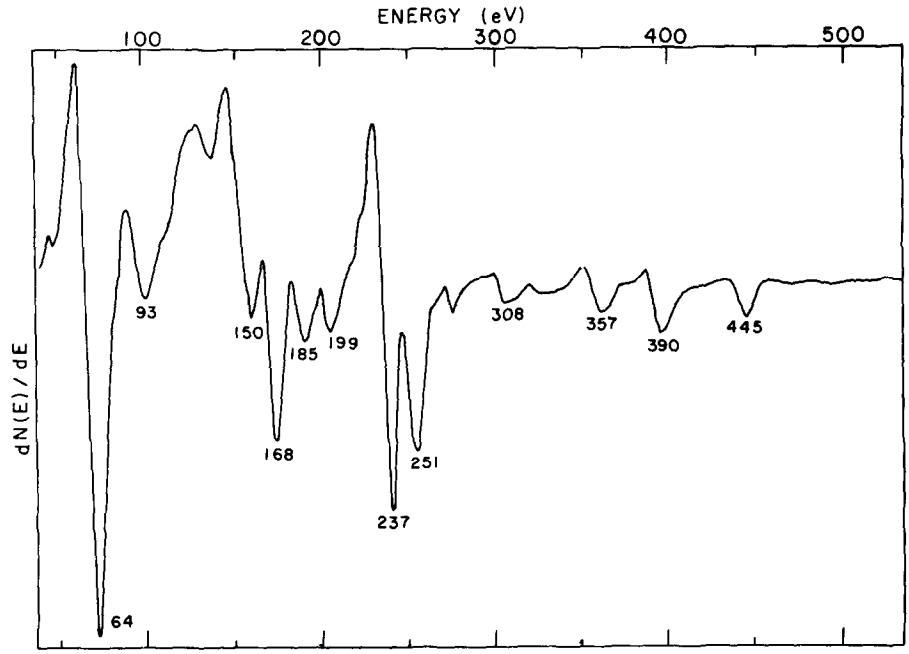

Fig. 1. AES spectrum of clean Pt(100)-(5 × 20) surface.

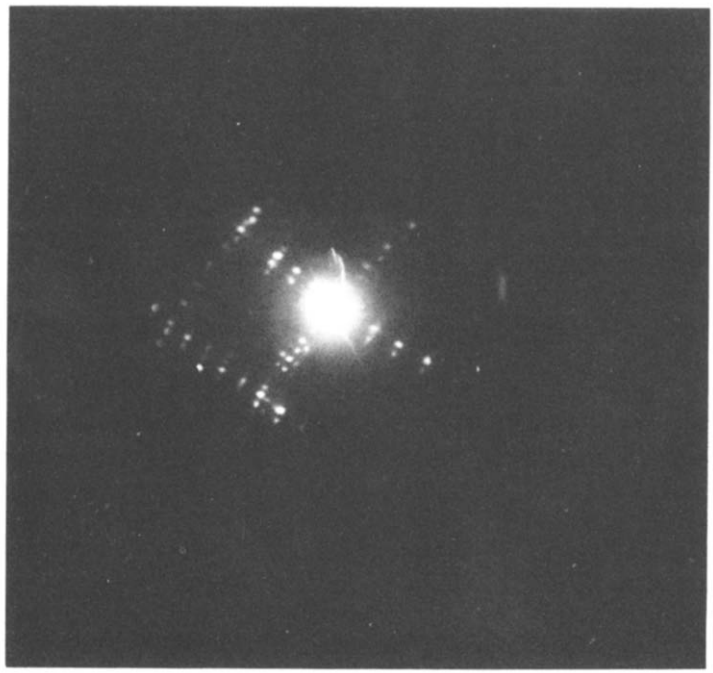

Fig. 2. (5 × 20) LEED pattern characteristic of the clean surface (beam energy = 64 eV).

annealing the sample at 1300 K in a background of oxygen. After the initial cleaning procedure annealing in oxygen was found to be sufficient to maintain a clean surface. A typical Auger spectrum of the clean surface is shown in fig. 1, and the (5 X 20) LEED pattern is shown in fig. 2.

Gases for adsorption were admitted into the vacuum chamber through a 22 gauge stainless steel needle connected to stainless steel manifold external to the chamber by a variable leak valve. The needle enabled the exposure of gases directly onto the front face of the sample to minimize background effects.

3. Results

3.1. Carbon monoxide adsorption and desorption

3.1.1. Pt(100)–(5 X 20)

The adsorption and desorption characteristics of CO on the Pt(100)-(5 X 20) surface were studied in order to characterize the surface and to provide a calibration of surface coverage for thermal desorption and ESCA measurements with other gases. In general, the results obtained were in good agreement with previous studies [2,9], and are described in detail below.

LEED–thermal desorption studies. As reported by Kneringer and Netzer [9] the LEED pattern observed during adsorption of CO on the Pt(100)-(5 X 20) surface progressed from the (5 X 20) to a p(1 X 1) to a c(4 X 2). The c(4 X 2) pattern disordered rapidly in the beam as also reported. The pattern obtained after disordering the c(4 X 2) was the same as that obtained from a surface at slightly less than saturation coverage: the $\frac{1}{2}$ order spots disappeared, and streaks were observed about $(\frac{1}{2}, \frac{1}{4})$ positions. This pattern was thus quite similar to those reported by Morgan and Somorjai [11] for disordering of the c(4 X 2) pattern by the electron beam.

The thermal desorption spectra following adsorption of CO on the Pt(100)-(5 X 20) surface at 300 K are shown as a function of coverage in fig. 3. The CO desorption spectrum was qualitatively similar to that reported by McCabe and Schmidt [2], however, only three peaks (α_1, α_2, α_3) were observed in this study. The additional desorption states reported by McCabe and Schmidt were observed only when the surface was contaminated with small amounts of carbon. Also, no evidence for the CO(β) states at 900 K reported by Morgan and Somorjai [11] was observed in the present study.

The three CO(α) states did not fill sequentially with increasing CO exposure as shown by the coverage variation in fig. 3, and the sequence of LEED patterns observed by heating the CO saturated surface to desorb one or more of the CO(α) states was *not* the same as that obtained by variation of the surface coverage for a fixed adsorption temperature. Following saturation of the surface with CO to form the c(4 X 2) structure, the CO(α_1) state was removed by heating the surface to 440 K and cooling to room temperature. A c(2 X 2) LEED pattern was then ob-

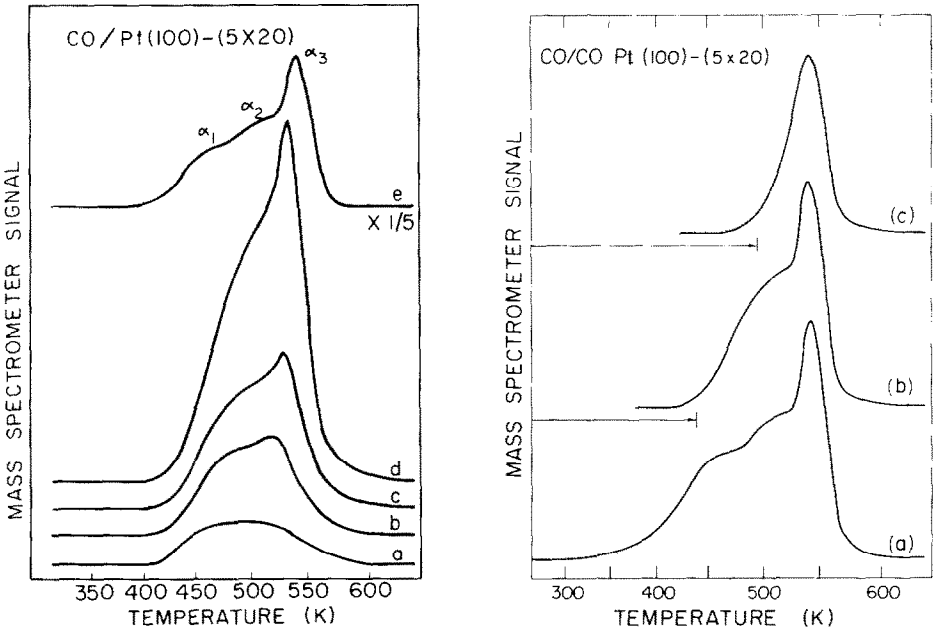

Fig. 3. Flash desorption spectra for CO/Pt(100)-(5 × 20): coverage variation exposure (a) 0.1 L, (b) 0.2 L, (c) 0.4 L, (d) 0.6 L, (e) 6.0 L.

Fig. 4. Flash desorption spectra for CO/Pt(100)-(5 × 20): partial flashes (a) T = 300 K, (b) T = 440 K, (c) T = 495 K.

served, and the α_2 and α_3 states desorbed upon further heating as shown in fig. 4. No relaxation of CO states occurred during the LEED observations and cooling of the sample to 300 K following the partial flashes (see fig. 4).

If the c(4 × 2) LEED patterns were assumed to correspond to a CO coverage of 75% of a monolayer [11] ($\alpha_1 + \alpha_2 + \alpha_3$ states), the coverage for the c(2 × 2) ($\alpha_2 + \alpha_3$ states) pattern obtained from thermal desorption was 0.52 monolayers and that for the p(1 × 1) pattern (α_3 state) was 0.28 monolayers. Thus, the coverage corresponding to the c(2 × 2) pattern obtained by thermal desorption was in good agreement with that which would be expected for such a pattern (0.5 monolayer), and the CO(α_3) state apparently corresponded to the random distribution of adsorbed CO on a (1 × 1) substrate at coverages up to $\frac{1}{4}$ monolayer. Calibrations of both CO and oxygen coverages were verified by XPS measurements as discussed in section 3.4. Finally, the LEED pattern returned to the (5 × 20) following the complete desorption of the CO(α) states upon heating the sample to 575 K.

Sticking probability measurements were also conducted using the high coverage LEED patterns above to calibrate surface coverages obtained from thermal desorp-

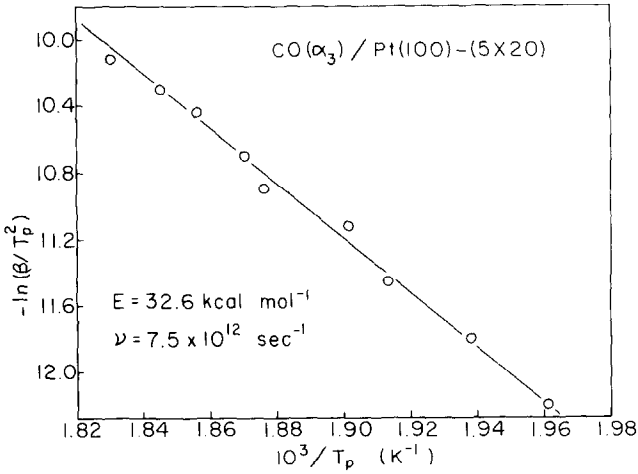

Fig. 5. Activation energy determination for $CO(\alpha_3)$/Pt(100)-(5 × 20).

tion measurements. The initial sticking probability of CO on the Pt(100)-(5 × 20) surface was approximately unity up to coverages of ~15% of a monolayer, at which a fall-off in the sticking probability was observed. A exposure of ~30 L was sufficient to saturate the surface. The initial sticking probability was somewhat higher than that reported by McCabe and Schmidt [2], although in both cases a fall-off was observed at ~20% of a monolayer.

The overlap of the three CO(α) states precluded direct determination of the desorption kinetics for each state. All three states were assumed to be first order, as the peak positions were independent of coverage. As previously mentioned, the α_3 state could be isolated by saturation of the surface with CO followed by heating the sample to 495 K to remove the α_1 and α_2 states. The activation energy for desorption of the $CO(\alpha_3)$ state was then obtained by heating rate variation methods (fig. 5), and the activation energy and pre-exponential factor for desorption were found to be

$$E_{\alpha_3} = 32.6 \text{ kcal/mole}, \quad \nu_{\alpha_3} = 7.5 \times 10^{12} \text{ s}^{-1},$$

for initial coverages of the α_3 state of 3.6 (±0.2) × 10^{14} molecules/cm^2. If it was then assumed that for all three CO(α) peaks

$$\nu_{\alpha_1} = \nu_{\alpha_2} = \nu_{\alpha_3} \approx 10^{13} \text{ s}^{-1},$$

the activation energies were found to be

E_{α_1} = 28.1 kcal/mole, T_p = 465 K;
E_{α_2} = 31.6 kcal/mole, T_p = 522 K;
E_{α_3} = 33.1 kcal/mole, T_p = 545 K;

based on the peak temperature for each state as listed above.

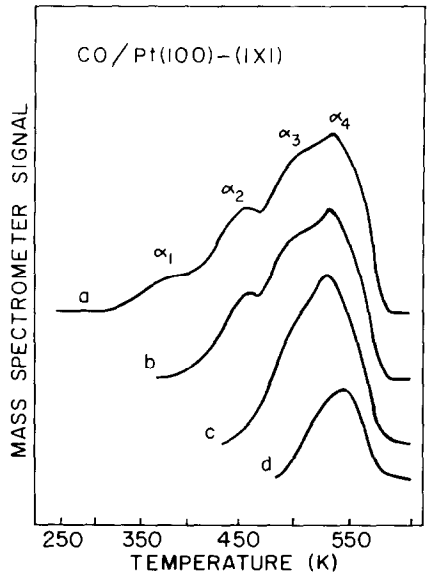

Fig. 6. Flash desorption spectra for CO/Pt(100)-(1 × 1): effect of adsorption temperature (a) T_a = 260 K, (b) T_a = 365 K, (c) T_a = 435 K, (d) T_a = 485 K.

3.1.2. Pt(100)-(1 × 1)

The CO desorption spectrum characteristic of CO adsorption on the Pt(100)-(1 × 1) [12] was obtained by adsorption of oxygen on the (5 × 20) surface followed by exposure to CO. CO reacted with adsorbed oxygen to form CO_2 which desorbed from the surface during exposure, and the CO adsorbed after depletion of the surface oxygen was monitored by thermal desorption *. The desorption spectra for CO adsorbed at several temperatures following the clean off reaction are shown in fig. 6. For adsorption of CO in this fashion at 300 K, four α states were observed; the LEED pattern prior to heating to produce curve (a) of fig. 6 was a c(4 × 2). When CO was adsorbed at higher temperatures, the surface could not be saturated with CO due to desorption of the lowest temperature states. At 365 K only the α_2, α_3, and α_4 states were observed, and the LEED pattern observed was a sharp $(\sqrt{2} \times 3\sqrt{2})R45°$ as reported by Brodén et al. [13] for less than saturation coverage of CO on the unreconstructed Pt(100) surface. At 435 K, only the α_3 and α_4 states were observed, and the corresponding LEED pattern was a c(2 × 2) also observed by Brodén et al. [13]. At 485 K, only the α_4 state remained on the surface,

* The adsorption of oxygen on the Pt(100)-(5 × 20) surface is discussed in the present work. Detailed kinetic studies of the CO oxidation reaction have also been performed and will be discussed in a future paper [5].

and a p(1 X 1) LEED pattern was observed. When this state was desorbed by heating the sample to 575 K, the LEED pattern returned to a (5 X 20). Further, as the sequence of LEED patterns observed in this study for adsorption of CO on a surface with increasing temperature (and decreasing CO coverage) was exactly the reverse of that observed by Brodén et al. [13] for increasing CO coverage on the Pt(100)-(1 X 1) surface, it is suggested that on this surface the CO(α) states did fill sequentially, in contrast to the (5 X 20) surface.

3.2. Oxygen adsorption on desorption on Pt(100)-(5 X 20)

Oxygen was observed to adsorb on the Pt(100)-(5 X 20) surface up to coverages of ~2/3 of a monolayer, in marked contrast to the failure reported by other workers in attempts to adsorb oxygen on this surface [1,8,11]. In the present study it was found that the principal barrier to achievement of high oxygen coverages on

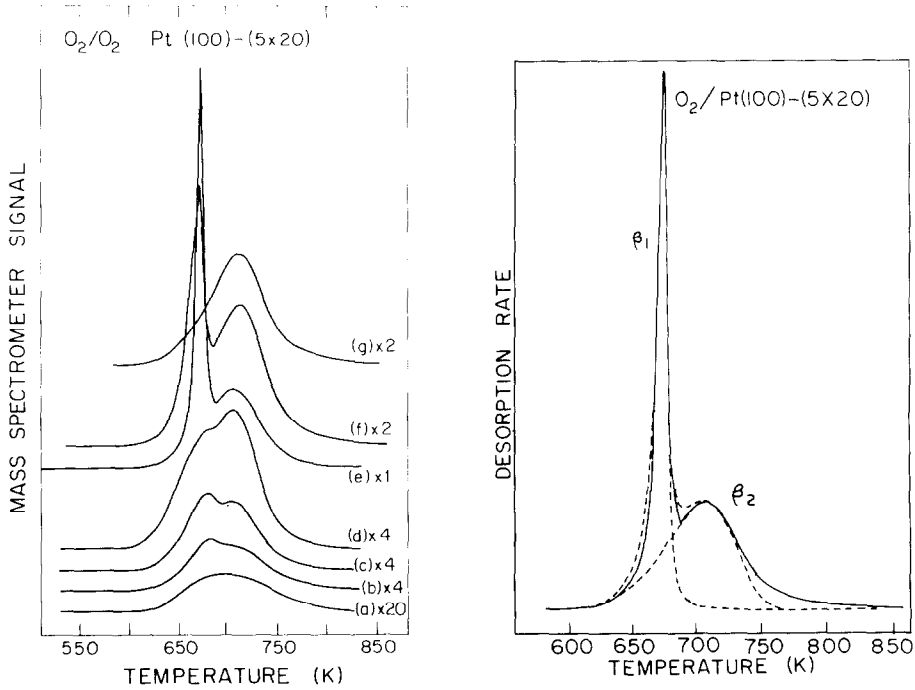

Fig. 7. Flash desorption spectra for O_2/Pt(100)-(5 X 20): effect of adsorption temperature (a) T_a = 300 K, (b) T_a = 505 K, (c) T_a = 534 K, (d) T_a = 562 K, (e) T_a = 585 K, (f) T_a = 607 K, (g) T_a = 635 K. Exposure ≈600 L.

Fig. 8. Flash desorption spectra for O_2/Pt(100)-(5 X 20), T_a = 585 K; (———) experimental data; (– – –) calculated curve (see text).

this surface was *not* an extremely low sticking probability for oxygen as suggested by other workers, but rather an efficient clean off reaction by background H_2 and CO. Oxygen adsorption was strongly dependent both upon the effective pressure of oxygen at the surface and upon the temperature of the Pt sample. As this result is quite different from that reported by other workers, a discussion of the exact procedure is in order here. Oxygen was dosed onto the sample surface through a 22 gauge stainless steel needle at background pressures of $\sim 10^{-7}$ Torr. Based on the measured pumping speed, a mass balance around the chamber yielded an effective pressure at the surface approximately 20 times greater than the total background pressure. Thus even with a background partial pressure of 10^{-9} Torr of species such as H_2 and CO which can "clean off" oxygen, the ratio of partial pressures, $(p_{H_2} + p_{CO})/p_{O_2}$ at the surface was less than 0.001. In spite of this large enhancement of the oxygen partial pressure at the surface, this technique was *not* sufficient by itself to achieve reproducibly high oxygen coverages. First, it was found to be necessary to evacuate the gas dosing manifold and recharge it with oxygen before *each* dose in order to minimize displacement of the impurities which contributed to the clean off reaction from the stainless steel walls. Second, and most importantly, it was necessary to maintain the Pt sample at elevated temperatures during oxygen dosing in order to inhibit the clean-off reaction. Bowker et al. [14] have shown that the CO oxidation reaction on silver exhibits a negative apparent activation energy due to the desorption of CO from the surface which competes with the oxidation reaction. A similar effect was observed on the Pt(100)-(5 X 20) surface at temperatures above 450 K for which at least one of the CO(α) states was unstable [5]. Thus by maintaining the Pt sample at the highest temperature at which adsorbed oxygen was still stable on the surface, the clean off reaction was minimized, and the adsorption of oxygen occurred most efficiently. The dramatic effect of surface temperature on the oxygen coverage achieved is shown in fig. 7 for adsorption of oxygen on the Pt(100)-(5 X 20) surface at temperatures between 300 K and 635 K. The coverage of oxygen increased by a factor of ~50 as the surface temperature was

Table 1
Oxygen coverage following exposure of the Pt(100)-(5 X 20) surface to 600 LO_2

Adsorption temperature (K)	Oxygen atom coverage (cm^{-2})
300	1.6×10^{13}
505	9.2×10^{13}
534	1.3×10^{14}
562	2.5×10^{14}
585	8.8×10^{14}
607	6.6×10^{14}
635	4.6×10^{14}

increased from 300 to 585 K (see table 1). Above 585 K, some of the oxygen desorbed during adsorption, and as shown in fig. 7 the coverage decreased above this temperature. Detailed measurements of the sticking probability of O_2 on the Pt(100)-(5 X 20) surface were not performed. However, using an enhancement factor of 20 over the background pressure for dosing of the surface through the needle as described, and assuming negligible clean off of oxygen from the surface by reaction, the *lower limit* of the sticking probability may be estimated from the *saturation* coverages and exposures to be 1×10^{-3} at 585 K.

Oxygen desorbed from the Pt(100)-(5 X 20) surface in the two peak spectrum shown in fig. 8 following adsorption at 585 K. This spectrum was quite reproducible, given the adsorption procedure outlined above, for exposure times of ~300 s. The two peaks, β_1 and β_2 each accounted for approximately half of the total oxygen adsorbed at 585 K; however, by adsorption of oxygen at higher temperatures the β_1 peak could be suppressed. At 635 K only the β_2 peak was present on the surface following saturation exposure to oxygen.

Several ordered LEED patterns were observed for oxygen adsorption on the Pt(100)-(5 X 20) surface. When the β_2 state alone was present on the surface, a p(1 X 1) pattern was observed. When a portion of the β_1 state was also present (this was achieved by adsorption of oxygen between 600–615 K, or by heating the oxygen saturated surface to 660 K and cooling), the (3 X 12) LEED pattern shown in fig. 9 was observed. Finally, when the surface was saturated with oxygen at 585 K, the LEED pattern shown in fig. 10 was observed. This pattern was not character-

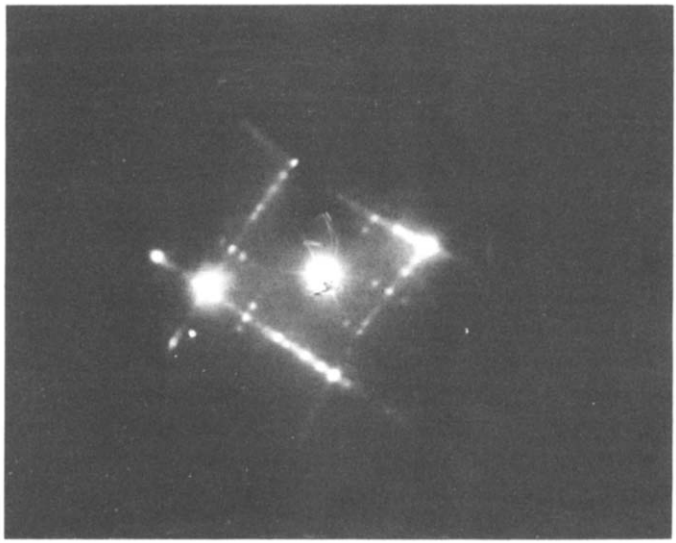

Fig. 9. (3 X 12) LEED pattern, obtained from absorbing oxygen at 585 K followed by flashing to 640 K (beam energy = 37 eV).

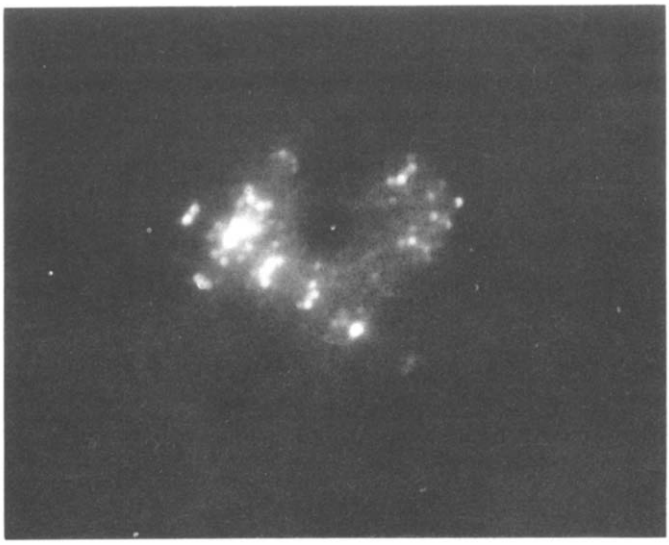

Fig. 10. LEED pattern: oxygen saturated Pt(100)-(5 × 20) surface, oxygen adsorbed at 585 K (beam energy = 37 eV).

ized, although it possesses major features in the 1/3 order positions as does the (3 × 12). Starting with an oxygen saturated surface, the (3 × 12) and p(1 × 1) patterns could be created by flashing the sample to 660 and 680 K, respectively, and the (5 × 20) pattern characteristic of the clean surface restored by heating to 750 K to desorb both oxygen states. No interconversion between the β_1 and β_2 states was observed for experiments in which the oxygen saturated surface was heated to desorb part or all of the β_1 state and cooled to room temperature.

The desorption kinetics for the $O_2(\beta_1)$ and $O_2(\beta_2)$ states were obtained by heating rate variation techniques [15] and from isothermal desorption measurements. The heating rate variation studies (see fig. 11) yielded apparent activation energies for the oxygen β_1 and β_2 states of 51.6 kcal/mole and 38.6 kcal/mole, respectively. However, it is clear that the extremely narrow β_1 peak cannot be described by a simple first order process, and the narrow width of the peak is suggestive of a process with a coverage dependent activation energy, observed as well for several other desorption/reaction systems [16,17]. In order to extract the coverage dependence of the oxygen β_1 peak, isothermal experiments were performed. In these experiments the sample was heated to the leading edge of the β_1 desorption peak, and the heater current was rapidly decreased in order to stabilize the sample temperature within ~2 s. This technique resulted in the isothermal desorption primarily of the $O_2(\beta_1)$ state. At the temperatures employed, the desorption rate for the β_2 state was small, and the β_2 state could be desorbed by again heating the sample after the isothermal desorption of the β_1 peak was complete. The sample

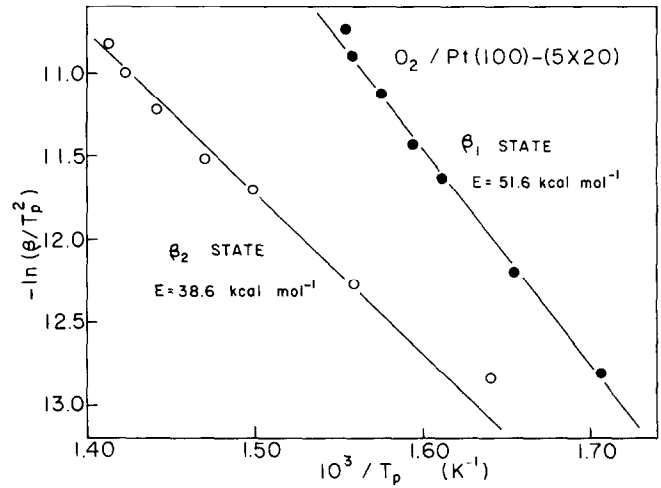

Fig. 11. Activation energy determination for O_2/Pt(100)-(5 × 20).

temperature and the isothermal desorption spectra are shown in fig. 12 for 642, 637 and 632 K, respectively (a, b, c). The isothermal desorption of the oxygen β_1 state shown in fig. 12 is indicative of an autocatalytic process; for a simple nth order process ($n \geqslant 0$) the isothermal rate cannot exceed the initial rate for any non-zero time. Further, the exponential decay once the rate has reached a maximum indicates that nth order processes with $n \leqslant 0$ are also inapplicable; such a process would yield an accelerating rate until the surface coverage was depleted, at

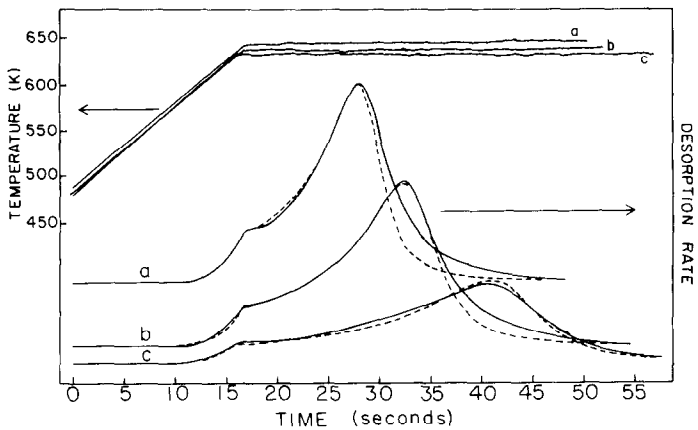

Fig. 12. Isothermal desorption spectra for the $O_2(\beta_1)$ state: (———) experimental data; (– – –) calculated from eq. (1) in text with n = 2.

which time the fall off would be a step function, not an exponential decay. Such autocatalytic behavior may be produced, however, if either n, ν, or E are functions of the surface coverage.

Rate laws of the form

$$r = \nu \exp(-(E + \omega c/c_0)/RT)\, c^n \tag{1}$$

have been successfully applied for first order autocatalytic reactions [16,17], and this form was chosen to express the coverage dependence for oxygen desorption from the β_1 state. In this case c and c_0 refer to the instantaneous and initial coverages of the β_1 state only. From the rate equation (1) above, plots of $\ln(r/c^n)$ versus c should yield straight lines of slope $-\omega/c_0RT$ for these isothermal experiments, provided the proper value is chosen for n. Fig. 13 shows plots of this type for n = 1 and n = 2, and the second order rate expression may be seen to fit the data well, yielding an interaction energy, ω, of ~7 kcal/mole. This rate law was then applied to thermal desorption data, and by trial and error fits of the peak temperatures and widths at half maximum for heating rates between 1 and 10 K/s, values of E, ν, and ω were calculated to be

$$E_{\beta_1} = 46.0 \text{ kcal/mole}, \quad \omega = 7.1 \text{ kcal/mole}, \quad \nu_{\beta_1} = 53 \text{ cm}^2/\text{molecule} \cdot \text{s}.$$

These values provided an excellent fit to both the thermal desorption and isothermal desorption experiments as shown in figs. 8 and 12.

The activation energy for the $O_2(\beta_2)$ peak was obtained by heating rate variation methods as previously described. Due to the overlap with the β_1 peak, no attempt

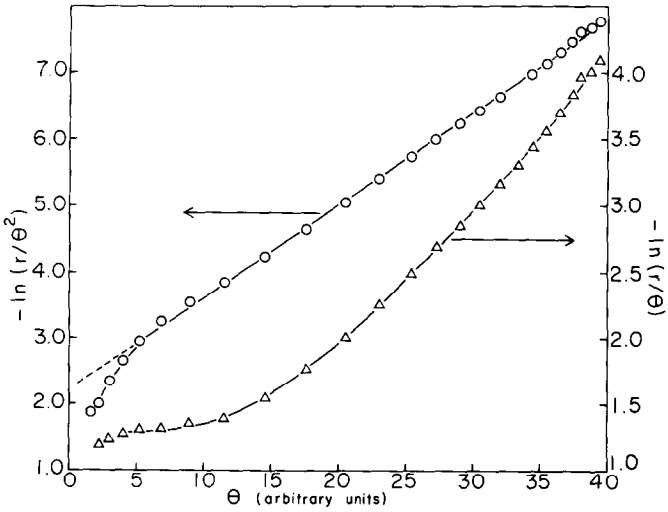

Fig. 13. Plots of $\ln(r/\theta)$ and $\ln(r/\theta^2)$ versus θ; isothermal oxygen desorption.

was made to analyze the peak shape, and the desorption kinetics were obtained by trial and error simulation of the thermal desorption measurements using the calculated activation energy in rate equations of differing order. A simple first order rate expression was found to provide the best fit as shown in fig. 8, for values of E_{β_2} and ν_{β_2} of

$E_{\beta_2} = 38.6$ kcal/mole, $\quad \nu_{\beta_2} = 2.6 \times 10^{11}\ s^{-1}$

It should be noted that the coverages of the β_1 and β_2 states used in the above rate equations were independent of each other, as no conversion between states was observed.

3.3. H_2 Adsorption and desorption on Pt(100)-(5 × 20)

The adsorption of hydrogen on the Pt(100)-(5 × 20) was found to be quite sensitive to the temperature of the platinum sample. At 300 K only two hydrogen states were present on the surface, with a total coverage of 1.3×10^{14} molecules/cm^2 determined from thermal desorption experiments by calibration of the mass spectrometer sensitivity relative to that for CO. No extra ordering of the LEED pattern was observed; at this point the pattern remained a (5 × 20). However, when the sample temperature was decreased to 200 K, the behavior was markedly different.

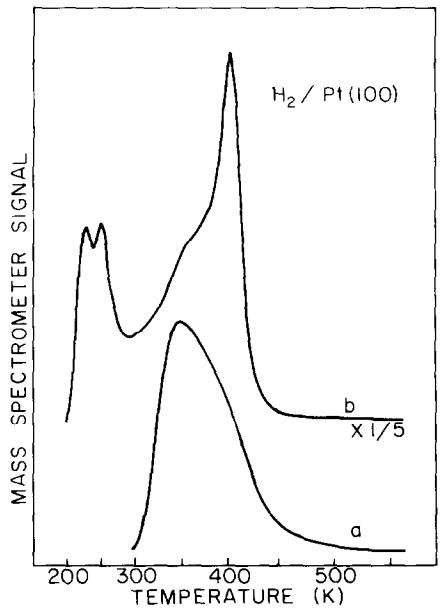

Fig. 14. Flash desorption spectra for H_2/Pt(100)-(5 × 20): effect of adsorption temperature (a) $T_a = 300$ K, (b) $T_a = 200$ K.

The magnitude of both of the peaks previously observed increased dramatically, and two new states were observed to desorb below 300 K (see fig. 14), similar to the results obtained by Lu and Rye on the unreconstructed Pt(100) surface [18]. The total hydrogen coverage in this case was 1.1×10^{15} molecules/cm^2 – a large increase in the amount of adsorbed hydrogen. In addition, the LEED pattern observed in this case was a p(1 X 1), not the (5 X 20) observed for adsorption at 300 K. After heating the hydrogen-saturated (1 X 1) surface to 300 K to desorb the two low temperature states, the LEED pattern remained a (1 X 1). In order to restore the (5 X 20) surface, it was necessary to desorb the higher temperature states as well, although extensive studies were not performed to determine whether this reconstruction required *complete* desorption of adsorbed hydrogen. Thus it was possible to reconstruct the Pt(100)-(5 X 20) surfaces to the p(1 X 1) structure by adsorption of hydrogen, however, the reconstruction exhibited a threshold temperature below 300 K above which the reconstruction could not be carried out. In addition, this reconstruction appears irreversible once the (1 X 1) structure is created; heating the sample above the threshold temperature did not reverse the process until nearly all of the hydrogen was desorbed.

3.4. XPS measurements

XPS measurements were performed to provide an independent check on the coverages of oxygen and carbon monoxide on Pt(100)-(5 X 20). Shown in fig. 15 are the spectra for the O(1s) level of adsorbed oxygen and carbon monoxide at saturation. The binding energy scale is referenced to the Pt($4f_{5/2}$) transition which has been measured to occur at 74 eV with respect to the Fermi level [19]. The relative O(1s) intensity of oxygen to carbon monoxide was measured to be 0.86 : 1.

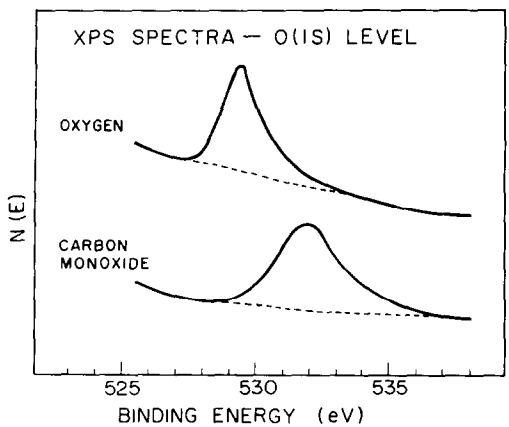

Fig. 15. O(1s) XPS spectra for adsorbed oxygen and carbon monoxide on Pt(100)-(5 X 20).

If the maximum CO coverage is taken to be 0.75 monolayer in correspondence with the c(4 × 2) LEED pattern, then the oxygen saturation coverage was 0.64 monolayer, in excellent agreement with the flash desorption results reported earlier. The observed electron binding energy difference of about 2 eV between oxygen and carbon monoide O(1s) levels was also in good agreement with the results on the unreconstructed Pt(100) surface [13].

4. Discussion

The differences in adsorption activity between the Pt(100)-(5 × 20) and (1 × 1) surface are clearly demonstrated by the present study. The Pt(100)-(5 × 20) surface was essentially an inactive surface; in those cases in which the surface remained "locked" into this structure, (e.g. O_2 and H_2 adsorption at 300 K), little adsorption took place. The activity of the (5 × 20) surface for adsorption lies in its ability to be converted back to the (1 × 1) structure by the presence of adsorbed species under certain conditions. Due to the fact that this conversion is not instantaneous upon adsorption of the first admolecules, but appears to require a threshold adsorbate concentration, the distribution of binding states observed in flash desorption studies for all of these species is different on the (5 × 20) and (1 × 1) surfaces, even though the (5 × 20) may be converted to the (1 × 1) during adsorption.

The effect was most clearly demonstrated in the case of CO adsorption. Although on both the (1 × 1) and (5 × 20) surfaces the LEED pattern at saturation coverage was a c(4 × 2), and although a p(1 × 1) pattern was observed for intermediate coverages of CO on the (5 × 20) surface, the desorption spectra from the two surfaces were different. The three CO(α) states on the (5 × 20) surface were also present on the (1 × 1) surface. However, the (1 × 1) surface exhibited a fourth, lower temperature peak, and the population of the other three states was different from that observed on the (5 × 20) surface. Further, on the (5 × 20) surface the CO binding states did *not* populate sequentially. In contrast, on the (1 × 1) surface it may be inferred from the equivalence of the partial desorption experiments in the present study and the coverage variation of Brodén et al. [13] that the CO binding states do populate sequentially; no reconstruction is necessary in order to accommodate adsorption on this surface.

The effect of hydrogen adsorption on the Pt(100) surface was quite similar to that of CO adsorption. Only small amounts of hydrogen could be adsorbed on the (5 × 20) surface; it was necessary to reconstruct the surface to the (1 × 1) structure if high coverages were to be achieved. In the case of hydrogen adsorption, however, this reconstruction did not occur as facilely as for CO adsorption. The surface had to be maintained at a low temperature during hydrogen adsorption in order to induce reconstruction. This observation is in contrast to most irreversible processes which exhibit a temperature threshold: such processes are generally activated, and the threshold is reached with increasing, rather than decreasing, temperature. It

appears therefore that for low coverages of hydrogen, the (5 X 20) and (1 X 1) surfaces may be in equilibrium with the (5 X 20) structure favored at higher temperature and the (1 X 1) at lower. When the temperature is decreased to favor the (1 X 1) structure, the surface has a much greater capacity for hydrogen adsorption, and this additional adsorption of hydrogen in turn stabilizes the (1 X 1) surface, effectively rendering the reconstruction irreversible. Thus, the reconstruction is not in itself irreversible, but the additional stabilization of the (1 X 1) surface due to increased hydrogen adsorption is the cause of the hysteresis in the surface structures observed as a function of temperature.

Several workers [1,8,11] studied the adsorption of oxygen on the Pt(100)-(5 X 20) surface, but reported that no detectable levels of oxygen were adsorbed. Kneringer and Netzer [9], however, were able to adsorb oxygen on the (5 X 20) surface up to coverages of $\frac{1}{4}$ monolayer with an initial sticking probability of 4×10^{-4}. They observed three desorption states for oxygen on the (5 X 20) surface with peak maxima at 790, 960, and 1070 K for heating rate of 30–40 K/s, which produced no change in the (5 X 20) pattern observed for the clean surface. In this work up to 2/3 of a monolayer of oxygen atoms could be adsorbed with an integrated-average sticking probability to saturation of 10^{-3}. In addition, the oxygen desorption spectrum exhibited only two peaks, an explosive, second order β_1 peak at 676 K, and a first order of β_2 peak at 709 K for a heating rate of 8.5 K/s. If the heating rates used by Kneringer and Netzer are substituted into the rate laws obtained in the present study, the peak temperatures of the β states calculated are ~700 and ~750 K, respectively, 40 to 90 K below the lowest temperature state they observed. Further, ordered LEED patterns were observed for oxygen adsorption on Pt(100)-(5 X 20) in the present study: a p(1 X 1) when only the β_2 state was present on the surface, a (3 X 12) and a more complex pattern when both states were present. Although extensive exposure variation studies were not performed, it appears from the adsorption–temperature-variation studies that the two oxygen β states did not fill sequentially; even at low coverages both states were present. As with CO adsorption on the (5 X 20) surface, oxygen is thus able to reconstruct the surface to the (1 X 1). However, the LEED patterns are different from those observed for adsorption initially on the (1 X 1) surface [8], implying that the structure of the oxygen adlayer is dependent upon the method of formation of the (1 X 1) substrate.

The kinetics for oxygen desorption from the Pt(100)-(5 X 20) surfaces are quite interesting in themselves. If oxygen is dissociatively adsorbed on this surface, it would be expected that the desorption would be characterized by a simple, second order recombination reaction. Yet neither the β_1 nor the β_2 state exhibited simple second order kinetics; the β_1 peak, though second order, exhibited a coverage dependent activation energy, and the β_2 peak was best fit by a simple first order model. It should be noted here that the overlap of the two peaks prevented a detailed kinetic study of the β_2 peak; it is likely that this peak could be fit by a second order model with very small interactions, however, a simple second order

model with an activation energy obtained by heating rate variation methods predicted a peak at least 50% too wide.

The thermal desorption results for oxygen clearly suggest the presence of attractive forces in the adlayer. In effect, the adsorbate becomes less stable as the coverage decreases, and this decrease in stability is reflected in a reduction of the activation barrier for associative recombination. The value of the interaction parameter, ω, determined from eq. (1) may be somewhat high, since eq. (1) was derived on the basis of the Bragg-Williams approximation. Nonetheless, it is apparent from the results that the desorption event is not simple; the β_1 and β_2 states do not follow the simple-order kinetics expected for atom recombination. Similar complex desorption kinetics were observed for oxygen on Ag(110) [21]. In that case, oxygen adsorbs in chains perpendicular to the close-packed rows of silver atoms; i.e., one-dimensional "islands" are formed, but desorption is not autocatalytic. Shigeishi and King [22] have suggested that oxygen adsorbs on Pt(111) in islands, and on Pt(100)-(5 X 20) the CO oxidation kinetics are best fit by assuming the oxygen adatoms to be in islands [5]. Further, from the LEED results accompanying oxygen adsorption, it is apparent that different surface oxygen phases form at different coverages. Thus oxygen desorption is accompanied by surface rearrangements which are undoubtedly cooperative phenomena. It is abundantly clear then that the autocatalytic desorption step is the result of attractive forces in the adlayer; the exact nature of these forces is not known. The complexity of this process precludes any simple interpretation of the frequency factor, ν_{β_1}.

Though the dominant temperature effect in promoting oxygen adsorption was probably the shorter CO surface lifetime at elevated temperatures, the importance of activated adsorption cannot be ruled out. If activated adsorption were the sole source of the low apparent sticking probability of O_2, however, it would be expected that the results obtained in different laboratories would be more consistent.

5. Conclusions

The Pt(100)-(5 X 20) surface was reconstructed to the (1 X 1) structure by adsorption of CO, H_2, or O_2. In the case of CO adsorption, the reconstruction was achieved quite easily at room temperature, although the distribution of CO binding states differed depending upon the initial surface structure. The H_2-induced reconstruction of the surface required surface temperatures below 300 K and exhibited a hysteresis with hydrogen coverage due to stabilization of the (1 X 1) surface by the induced adsorption of hydrogen which accompanied the structural change. Oxygen was adsorbed on the Pt(100)-(5 X 20) surface up to coverages of 2/3 of a monolayer with a net sticking probability of 10^{-3}. The major barrier to achieving high oxygen coverages is a facile clean off of oxygen via oxidation of background CO; this effect was suppressed by increasing the surface temperature. Oxygen also

induced a reconstruction of the (5 X 20) surface back to the (1 X 1) and additional ordered LEED structures were observed for oxygen coverages greater than ~1/3 monolayer. The desorption of oxygen adsorbed on the Pt(100)-(5 X 20) surface exhibited complex kinetics, as strong attractive interactions were observed within the oxygen–surface complex.

Acknowledgement

The authors gratefully acknowledge the support of the National Science Foundation through Grant NSF Eng 12964.

References

[1] C.R. Helms, H.P. Bonzel and S. Kelemen, J. Chem. Phys. 65 (1976) 1773; and references therein.
[2] R.W. McCabe and L.D. Schmidt, Surface Sci. 66 (1977) 101.
[3] H. Hopster, H. Ibach and G. Comsa, J. Catalysis 46 (1977) 37.
[4] H.P. Bonzel and J.J. Burton, Surface Sci. 52 (1975) 223.
[5] M.A. Barteau, E.I. Ko and R.J. Madix, Surface Sci., to be published.
[6] H.B. Lyon and G.A. Somorjai, J. Chem. Phys. 46 (1967) 2539.
[7] J.J. McCarroll, Surface Sci. 53 (1975) 297.
[8] G. Pirug, G. Brodén and H.P. Bonzel, in: Proc. 7th Intern. Vacuum Congr. and 3rd Intern. Conf. on Solid Surfaces, Vienna, 1977, p. 907.
[9] G. Kneringer and F.P. Netzer, Surface Sci. 49 (1975) 125.
[10] J.B. Benziger and R.J. Madix, Surface Sci. 94 (1980) 119.
[11] A.E. Morgan and G.A. Somorjai, Surface Sci. 12 (1968) 405.
[12] C.R. Helms, private communication.
[13] G. Brodén, G. Pirug and H.P. Bonzel, Surface Sci. 72 (1978) 45.
[14] M. Bowker, M.A. Barteau and R.J. Madix, Surface Sci. 92 (1980) 528.
[15] J. Falconer and R.J. Madix, Surface Sci. 48 (1975) 393.
[16] J.B. Benziger and R.J. Madix, Surface Sci. 79 (1979) 393.
[17] M.A. Barteau, M. Bowker and R.J. Madix, Surface Sci. 94 (1980) 303.
[18] K.E. Lu and R.R. Rye, Surface Sci. 45 (1974) 677.
[19] K. Siegbahn, C. Nordling, C. Johansson, J. Hedman, P.F. Heden, K. Hamrin, U Gelius, T. Bergmark, L.O. Werme, R. Manne and Y. Baer, in: ESCA Applied to Free Molecules (North-Holland, Amsterdam, 1969).
[20] H.P. Bonzel and G. Comsa, Vide 189 (1977) 130.
[21] H.A. Engelhart and D. Menzel, Surface Sci. 57 (1976) 591.
[22] R.A. Shigeishi and D.A. King, Surface Sci. 75 (1978) L397.